Annales Geophysicae (2004) 22: 4071–4076
SRef-ID: 1432-0576/ag/2004-22-4071

Annales Geophysicae

High altitude large-scale plasma waves in the equatorial electrojet at twilight

J. L. Chau[1] **and D. L. Hysell**[2]

[1]Radio Observatorio de Jicamarca, Instituto Geofísico del Perú, Lima, Peru
[2]Department of Earth and Atmospheric Sciences, Cornell University, Ithaca, New York, USA

Received: 7 April 2004 – Revised: 24 July 2004 – Accepted: 25 August 2004 – Published: 22 December 2004

Abstract. Jicamarca radar observations of a new class of large-scale plasma waves in the equatorial electrojet (EEJ) are presented and characterized. The study is based on long-term (204 days), single-baseline interferometry observations made in 2003 using a low-power radar mode, also known as JULIA mode, along with a few hours of observations made in an aperture synthesis imaging mode. The large-scale waves are found to occur at high altitudes in the E-region, mainly between 120 and 140 km, around twilight (between 18:30 and 20:00 LT), with durations of a few minutes to an hour. In our long-term observations, these large-scale waves occur very often (between 1 and 5 out 10 nights), drift westward ($\sim$70 ms^{-1}), exhibit very narrow spectral widths, and have both positive and negative Doppler shifts. The imaging results show that the large-scale waves occur along tilted bands that sweep westward and downward ($\sim$30–60 ms^{-1}), with a horizontal separation between bands of about 10–15 km. The cause of the waves remains unknown.

Key words. Ionosphere (ionospheric irregularities; equatorial ionosphere; instruments and techniques)

1 Introduction

This paper presents individual and statistical observations of a class of large-scale plasma waves in the equatorial electrojet not previously recognized or predicted. These waves occur at high altitudes of the EEJ region around twilight. Large-scale waves were first detected in the equatorial electrojet (EEJ) in the early 1980s in interferometry data from Jicamarca (Kudeki, 1983) and are now believed to dominate the structure and dynamics of the whole region. In recent years, large-scale waves have undergone numerous theoretical and numerical investigations (e.g. Farley, 1985; Kudeki et al., 1985; Ronchi, 1990; Hu and Bhattacharjee, 1998, for reviews). The theory of daytime waves in particular has matured to the point of driving the development of new experimental techniques to validate it (e.g. Kudeki and Sürücü, 1991; Hysell and Chau, 2002).

Large-scale waves in the nighttime EEJ are poorly understood by comparison. Nonlocal, nonlinear, and anomalous effects need to be considered in any meaningful analysis of the waves, and numerical simulations must be able to cope with steep wind shears and conductivity gradients in order to provide a complete description of the waves at night. Such analyses are hampered by our inability to measure plasma density, electric field, and neutral wind profiles directly in the electrojet region using ground-based remote sensing techniques.

If the nighttime large-scale EEJ waves are poorly understood, the twilight high altitude EEJ echoes are not understood at all. As we show below, these waves are frequently observed with the JULIA (Jicamarca Unattended Long-term Investigations of the Atmosphere) mode at Jicamarca, and there have also been a number of observations made recently using interferometry with multiple baselines (Hysell and Chau, 2002). However, very little attention has been devoted to characterizing or interpreting these observations until now.

Much of what is known about large-scale EEJ waves has been discovered using coherent scatter radars. However, measurements from conventional, monostatic, fixed-beam radars are inherently ambiguous; spatial and temporal variations in the scattering medium generally cannot be distinguished unless the velocity of the scatterers transverse to their line of sight is known, and features with scale sizes smaller than the radar illuminated volume cannot be resolved. Radar interferometry, using a single baseline, mitigates these problems to some degree. However, a clearer picture of what is going on inside the radar illuminated volume can be obtained by using interferometry with multiple baselines and aperture synthesis imaging techniques.

Radar imaging was introduced at Jicamarca by Kudeki and Sürücü (1991) to study the EEJ irregularities by using multiple receiving baselines. Later, Hysell, (1996) and Hysell and Woodmann (1997) improved the technique to study equatorial spread *F* (ESF) irregularities. Briefly, the main

Correspondence to: J. L. Chau
(chau@geo.igp.gob.pe)

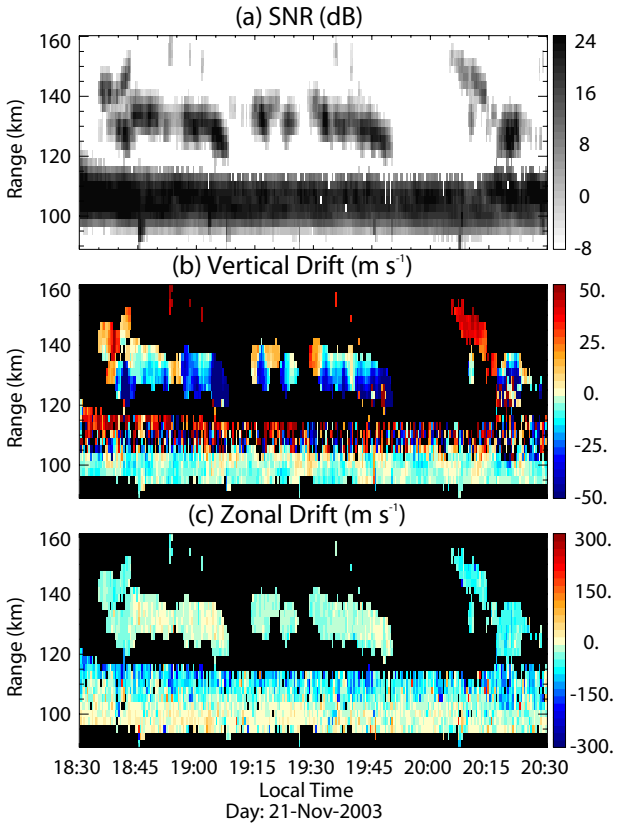

Fig. 1. JULIA EEJ observations around twilight on 21 November 2003. **(a)** Range-time intensity, **(b)** Doppler velocity, and **(c)** zonal drift. Note the occurrence of echoes above 120 kms.

purpose of the aperture synthesis imaging techniques is to estimate images of the ionosphere from second moment statistics of a finite number of sampling points on the ground (visibility function). The brightness and visibility terminology comes from the radio astronomy field, where aperture synthesis imaging techniques have been applied for quite some time. We recommend reading Woodman (1997) for a general review of the mathematical relationship between the statistical covariance of the visibility function and that of the brightness distribution to be imaged.

This paper begins with the presentation of long-term radar measurements performed in 2003. The results of a few hours of observations obtained with an aperture synthesis radar imaging mode are then presented and discussed. Finally, the statistical behavior and morphological characteristics of the high-altitude EEJ echoes are summarized.

2 Radar observations

Our studies are based on long-term (204 days) observations taken in 2003 using the low-power JULIA Doppler interferometer mode along with a few hours of radar observations made using an aperture synthesis imaging mode. Below, we describe the main results obtained with both modes.

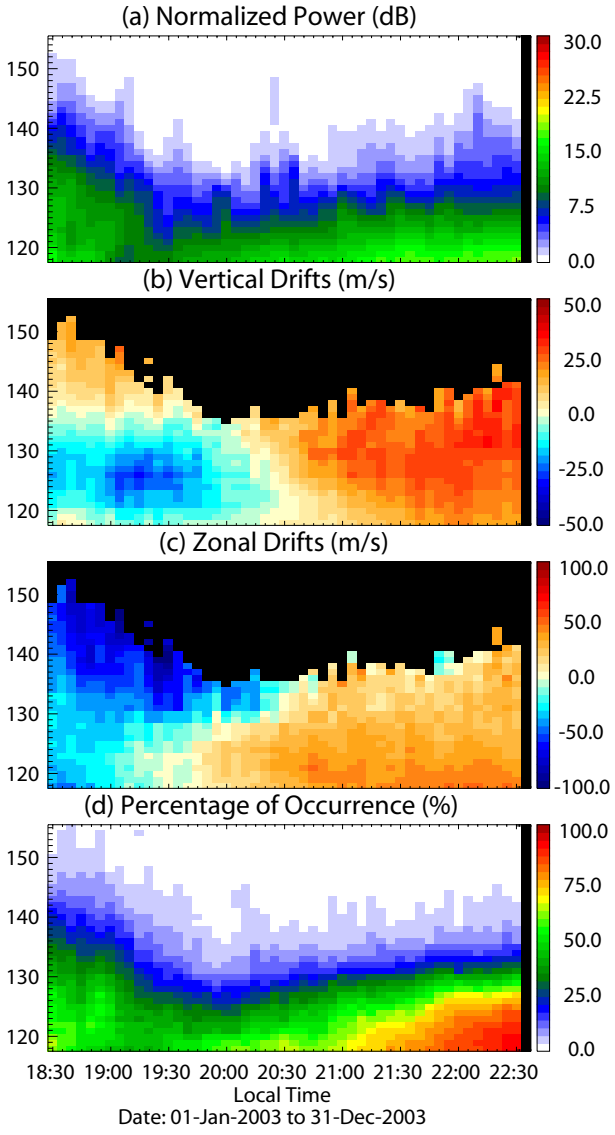

Fig. 2. Statistical results based on 204 days of single-baseline interferometry observations in 2003. **(a)** Normalized power, **(b)** Doppler velocities, **(c)** zonal drifts, and **(d)** percentage of occurrence.

2.1 JULIA interferometric observations

Begun in 1996, JULIA mode observations combine low-power transmitters with the main Jicamarca array for long-term studies of ionospheric and atmospheric phenomena (e.g. Hysell et al.,1997; Hysell and Burcham, 1998, 2002). In recent years, a variety of configurations have been added to the JULIA modes that utilize different antenna pointing positions and/or small sets of antennas, particularly for EEJ studies (e.g. Hysell and Burcham, 2002b; Hysell et al., 2002). The results presented here are based on a mode that has been used mainly to study ESF irregularities. Fortunately, this mode acquires data down to 85 km altitudes, allowing for observations of the EEJ irregularities as well.

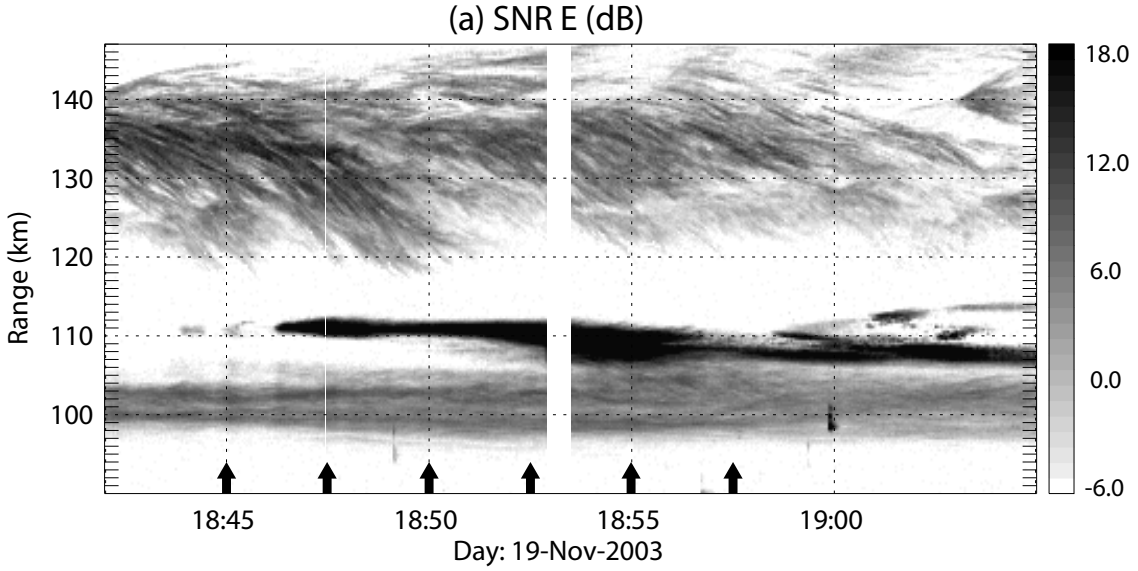

Fig. 3. Range-time intensity plot of the EEJ echoes observed on 19 November 2003 using an aperture synthesis imaging mode. The vertical arrows indicate where the snapshots shown below were taken.

For the mode in question, the north and south quadrants of the antennas are used for transmission. On reception, the west and east quadrants are used separately, forming an east-west interferometry baseline separated by ∼203.65 m. All four quadrants point perpendicular to the magnetic field lines at E- and F-region heights. The main observing parameters are: sampling range of 2.5 km, transmitter peak power of 40 kW, an interpulse period (IPP) that varies between 1500 and 2000 km, and a sampling window that starts at 85 km.

In Fig. 1 we show an example of JULIA EEJ echoes around twilight observed on 21 November 2003. From top to bottom, we show the range-time-intensity, Doppler velocity, and zonal drift of the echoes. As mentioned above, this observing mode is mainly for ESF studies and consequently has relative poor range (2.5 km) and time (64 s) resolution for E-region investigations. The echoes of interest in this study are those occurring above 120 km, which are patchy and drift westward. Their Doppler shifts can be both positive and negative.

Such echoes are common features in the JULIA-mode data. In Fig. 2 we summarize the statistical results of 204 days of observations in 2003 pertaining to: (a) power, (b) Doppler velocity, (c) zonal drift, and (d) percentage of occurrence. Based on these statistics, the high altitude twilight EEJ echoes present the following characteristics:

– They occur mainly before 20:00 LT and between 120 and 140 km.

– They drift westward, with the highest echoes (above 130 km in particular) drifting the fastest.

– The higher echoes (above 130 km) mainly have negative Doppler shifts (denoting ascent) while the lower echoes (between 120 and 130 kms) mainly have positive Doppler shifts.

– These echoes are very common. Between 18:30 and 19:00 LT they are expected to occur 3 to 5 out of 10 nights between 120 and 130 km, and 1 to 3 out of 10 nights between 130 and 145 km.

2.2 Aperture synthesis imaging observations

Figure 3 shows an example of EEJ echoes observed at twilight with very good range (300 m) and temporal resolution (4 s) over Jicamarca on 19 November 2003. The data were collected using a high-power (1 MW peak) transmitter and with 300 m (2 μs) uncoded pulses. The interpulse period was 225 km. Although not shown here, conventional spectral and interferometric analysis shows that the high altitude echoes present a very narrow spectral width (less than 70 ms^{-1}) compared to normal EEJ echoes, have downward phase velocities of ∼40 ms^{-1}, and drift westward at ∼70 ms^{-1}. The relatively long duration of this event is remarkable – the other events in our database were sporadic and lasted for a few minutes only.

The radar configuration during this experiment was similar to that described in the companion paper (Hysell et al., 2004) but with a different interpulse period. Briefly, transmission was performed with two quarters, with a broad antenna pattern of ±4°. Reception was performed on 8 receiving antennas, 6 using pre-existing Jicamarca modules (64ths), and 2 using smaller Yagi arrays specially built for these observations. The new Yagi arrays were added in order to have a shorter baseline compared to imaging experiments performed before (e.g. Hysell and Woodman, 1997; Hysell and Chau, 2002), increasing the unambiguous angular field

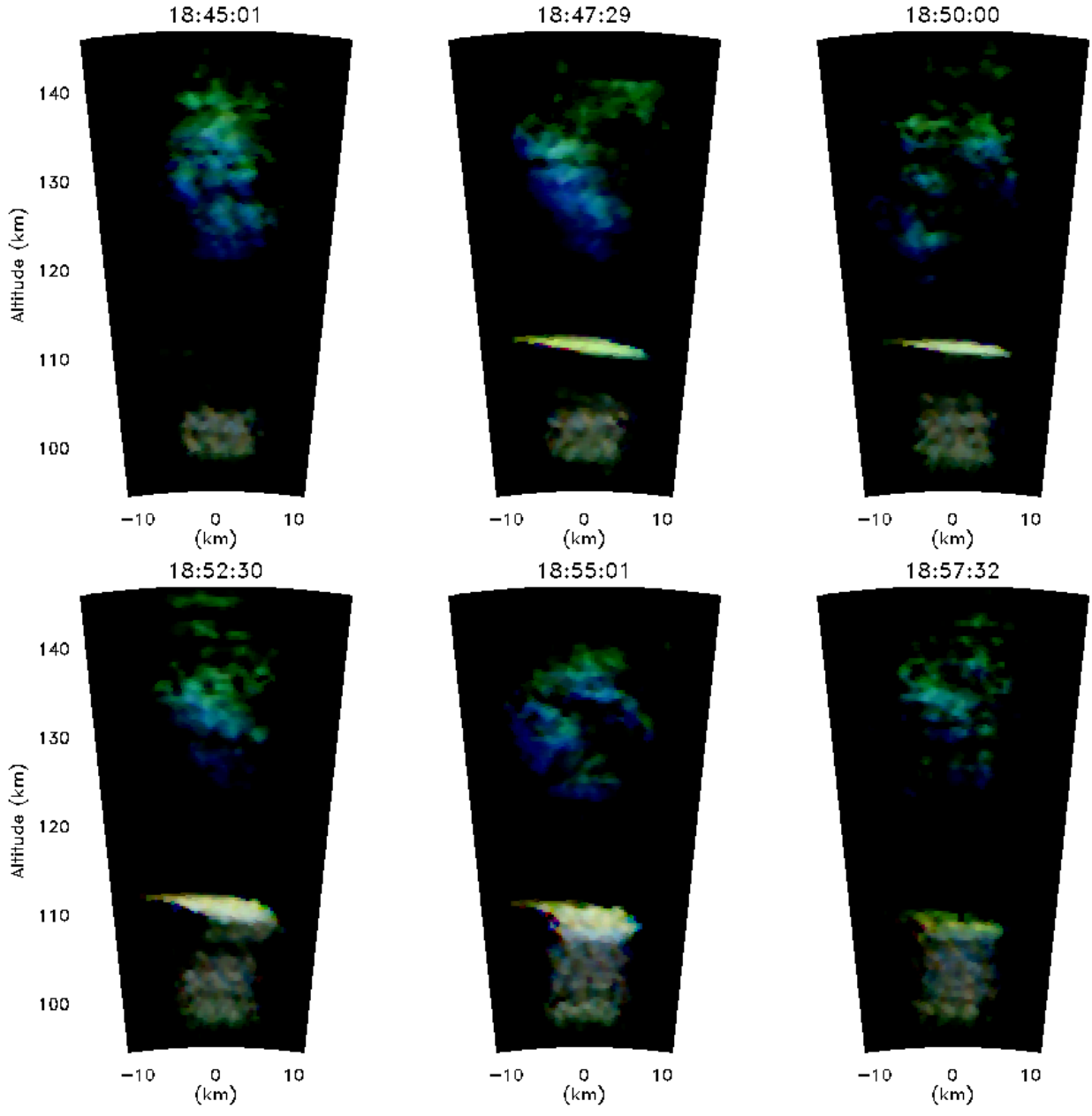

Fig. 4. Aperture synthesis images of high-altitude EEJ echoes observed around twilight on 19 November 2003 at six different local times. The vertical and horizontal axes of each snapshot represent the altitude and East-West (West to the left) distance in kilometers.

of view from $\pm 6.8°$ to $\pm 13.6°$. The Yagi arrays have a different antenna pattern than the Jicamarca modules, and our aperture synthesis imaging technique has been modified accordingly to take this effect into account.

One important step in processing radar signals from multiple antennas is the phase calibration procedure (e.g. Palmer et al., 1996). In previous Jicamarca imaging experiments, the phase calibration was performed by finding the phases that optimized the resulting ionospheric images in the sense of artifact minimization. This time, we have used the strong signal from the radio star Hydra ($\sim$9h17.8′ RA, $\sim -12°5'$Dec) to calibrate the phases of the 8-receiver antenna system. At the time of the experiment, Hydra passed over Jicamarca before sunrise when ionospheric scintillations are usually very weak, providing signals of very good quality. A similar procedure was adopted by Woodman (1971) but using antenna quarters instead of modules. Palmer et al. (1996) has also used a radio star (Cygnus A) to calibrate receiving modules at the MU radar.

In atmospheric radar imaging work, two high-resolution imaging techniques are commonly used: Capon's method (e.g. Palmer et al., 1998; Hysell and Burcham, 2000a) and

Maximum entropy (e.g. Hysell and Woodman, 1997). Both are adaptive, and both can be considered "super-resolution" methods, since the resolution of the images produced is not inherently limited by the Nyquist sampling theorem (e.g. Stoica and Moses, 1997). The advantages and disadvantages of both methods have been discussed by Chau and Woodman (2001) and Yu et al. (2000). Given the high number of baselines and the high signal-to-noise ratio of the EEJ signals, we considered Capon, which is computationally expedient, an appropriate means of obtaining radar images for these studies.

Radar images of the 19 November 2003 event around twilight are shown in Fig. 4. These snapshots were derived from data received on the 8 spatially separated antennas and the 28 associated cross-spectra for every range gate. The six images are snapshots computed from 4-s incoherent integrations and spaced by about 2.5 min. The time of the snapshots is indicated with vertical arrows in Fig. 4. The vertical and horizontal axes of each image panel represent the altitude and east-west distance in kilometers. The brightness of each pixel represents the signal-to-noise ratio on a log scale. Since Jicamarca operates at $\sim$50 MHz, the brightness is an indication of the intensity of 3-m irregularities, which then act as tracers of intermediate- and large-scale waves. Note that large and intermediate plasma waves are used differently for the E- and F-regions. In the E-region large-scale plasma waves have wavelengths of few kilometers, while intermediate scale plasma waves have wavelengths of hundreds of meters.

The hue represents the Doppler shift, with red- and blue-shifted echoes being color coded accordingly on a continuous color scale. The saturation represents spectral width, with pure and pastel colors signifying narrow and broad spectra, respectively. As we mentioned above, the high altitude EEJ echoes present very narrow spectral widths compared to the lower EEJ echoes, and we therefore computed images representing Doppler information between -120 and 120 ms^{-1}.

The images show the presence of the well-known EEJ echoes below 115 km with typical characteristics, i.e. alternating blue and pink bands propagating westward, representing the alternating phases of primary gradient drift waves with wavelengths of a few km (e.g. Hysell and Chau, 2002). The bands are more distinct between 97 and 107 km. A strong layer consisting of intermediate-scale waves appears around 18:46 LT.

The high-altitude EEJ irregularities appear between 130 and 140 km, arranged in narrow, tilted bands that drift downward ($\sim 30-60\,\mathrm{ms}^{-1}$) and westward. Inside the bands, secondary kilometer-scale waves are evident. Moreover, the bands are clustered, with separation between bands of $\sim 10-15$ km. The irregularities disappear when they arrive at an apparent altitude threshold of $\sim$118 km. Finally, irregularities above 132 km present smaller Doppler shifts (note the tendency for a green hue instead of blue), although they drift horizontally almost at the same velocity as those from lower altitudes.

3 Discussion and concluding remarks

Similar images have been shown by Hysell and Chau (2002) but with a narrower field of view. As pointed out in a previous section regarding JULIA observations, this phenomenon occurs very often. The source of these echoes has not been determined. As in Hysell and Chau (2002), we tentatively associate them with a gradient drift or interchange instability driven by the horizontal conductivity gradients and vertically upward electrojet currents known to be present in the vicinity of the solar terminator. Haerendel and Eccles (1992) explain the pre-reversal enhancement of the zonal electric field in terms of a current system generated in the vicinity of the evening solar terminator. Here, an enhanced vertical electric field arises below the F peak to drive Pedersen currents in the valley region that feed the dynamo current at F region heights. Westward $\boldsymbol{E}\times\boldsymbol{B}$ plasma drifts associated with the enhanced field are commonly observed in the bottomside F-region around twilight and, combined with the resulting pre-reversal enhancement of the vertical drifts, constitute the phenomenon known as the evening vortex (Kudeki and Bhattacharyya, 1999).

In combination with the zonal conductivity gradients near the terminator, the vertical currents in the valley and upper E-region may incite a combined gradient-drift interchange instability in the altitude region where the ions are marginally magnetized. That the observed irregularities occur near the altitude where the ion collision and gyrofrequencies match and, therefore, where the ion Pedersen mobility is greatest, suggests that such a mechanism may be operating. Further evidence comes from the fact that the irregularities cease to be observed by the time of the evening reversal, when zonal conductivity gradients are diminished. Quantitative analysis and modelling of the stability of the upper E- and valley regions around twilight will be undertaken in future work.

We have used conventional interferometry data and a few hours of radar imaging observations to characterize the still enigmatic high altitude EEJ echoes that occur very often at twilight over Jicamarca. From the long-term observations, these high altitude echoes are seen to occur very often (between 1 and 5 out of 10 nights) between 18:30 and 20:00 LT and above 120 kms, drift mainly westward and downward ($\sim 30-60\,\mathrm{ms}^{-1}$), and have both positive and negative Doppler shifts, depending on their altitude.

The imaging results reveal that these irregularities emerge first at high altitudes, where ions are marginally magnetized, and then sweep continuously downward and westward. Moreover, they are organized in tilted bands separated by $10-15$ km, which themselves show secondary kilometer scale wave generation. The bands vanish when they drift below a threshold altitude of about 118 km. In general, downward motion is observed below 132 km.

Although this phenomenon is very common, a quantitative study is require to understand its origin. Such a study will require precise specification of the conductivity gradients, currents, winds, and electric fields in the vicinity of the solar terminator. This complementary information could be

obtained by sounding rocket experiments or by combining the imaging techniques with other radar techniques to measure zonal EEJ winds (Hysell et al., 2002), EEJ density profiles (Hysell and Chau, 2001), and electric fields (Kudeki et al., 1999).

Acknowledgements. J. L. Chau wishes to thank W. Coles and R. Woodman for their insightful suggestions during the phase calibration procedures using Hydra. This work was supported by the National Science Foundation through cooperative agreement ATM-9911209 to Cornell University and by NSF grant ATM-0225686 and NASA grant NAG5-12164 to Cornell University. The help of the staff, particularly D. Scipion, H. Pinedo, and G. Vera, was much appreciated. The Jicamarca Radio Observatory is operated by the Instituto Geofísico del Perú, with support from the NSF Cooperative Agreement ATM-9911209 through Cornell University.

Topical Editor M. Lester thanks C. Haldoupis and another referee for their help in evaluating this paper.

References

Chau, J. L. and Woodman, R. F.: Three-Dimensional Coherent Radar Imaging at Jicamarca: Comparison of Different Inversion Techniques, J. Atmos. Sol. Terr. Phys., 63, 253–261, 2001.

Farley, D. T.: Theory of Equatorial Electrojet Plasma Waves: New Developments and Current Status, J. Atmos. Sol. Terr. Phys., 47, 729–744, 1985.

Haerendel, G. and Eccles, J. V.: The Role of the Equatorial Electrojet in the Evening Ionosphere, J. Geophys. Res., 97, 1181–1192, 1992.

[Hu and Bhattacharjee(1998)]Hu1998 Hu, S. and Bhattacharjee, A.: Two-Dimensional Simulations of Gradient-Drift Trubulence in the Daytime Equatorial Electrojet, J. Geophys. Res., 103, 20 749–20 759, 1998.

Hysell, D. L.: Radar Imaging of Equatorial *F* Region Irregularities with Maximum Entropy Interferometry, Radio Sci., 31, 1567–1578, 1996.

Hysell, D. L. and Burcham, J. D.: JULIA Radar Studies of Equatorial Spread *F*, J. Geophys. Res., 103, 29 155–29 167, 1998.

Hysell, D. L. and Burcham, J. D.: The 30-MHz Radar Interferometer Studies of Midlatitude *E* Region Irregularities, J. Geophys. Res., 105, 12 797–12 812, 2000a.

Hysell, D. L. and Burcham, J. D.: Ionospheric Electric Field Estimates from Radar Observations of the Equatorial Electrojet, J. Geophys. Res., 105, 2443–2460, 2000b.

Hysell, D. L. and Burcham, J. D.: Long Term Studies of Equatorial Spread F Using the JULIA Radar at Jicamarca, J. Atmos. Sol. Terr. Phys., 64, 1531–1543, 2002.

Hysell, D. L. and Chau, J. L.: Inferring *E* Region Electron Density Profiles at Jicamarca from Faraday Rotation of Coherent Scatter, J. Geophys. Res., 106, 30 371, 2001.

Hysell, D. L. and Chau, J. L.: Imaging Radar Observations and Nonlocal Theory of Large-Scale Waves in the Equatorial Electrojet, Ann. Geophys., 20, 1167–1179, 2002.

Hysell, D. L. and Woodman, R. F.: Imaging Coherent Backscatter Radar Observations of Topside Equatorial Spread *F*, Radio Sci., 32, 2309–2320, 1997.

Hysell, D. L., Larsen, M. F., and Woodman, R. F.: JULIA Radar Studies of Electric Fields in the Equatorial Electrojet, Geophys. Res. Lett., 24, 1687–1690, 1997.

Hysell, D. L., Chau, J. L., and Fesen, C. G.: Effects of Large Horizontal Winds on the Equatorial Electrojet, J. Geophys. Res., 107, doi:10.1029/2001JA000217, 2002.

Hysell, D. L., Chun, J., and Chau, J. L.: Bottom-type scattering layers and equatorial spread *F*, Ann. Geophys., 22, 4061–4069, 2004.

Kudeki, E.: Plasma Turbulence in the Equatorial Electrojet, Ph.D. thesis, Cornell University, Ithaca, New York, 1983.

Kudeki, E. and Bhattacharyya, S.: Postsunset Vortex in Equatorial *F*-Region Plasma Drifts and Implications for Bottomside Spread-*F*, J. Geophys. Res., 104, 28 163–28 170, 1999.

Kudeki, E. and Sürücü, F.: Radar Interferometric Imaging of Field-Aligned Plasma Irregularities in the Equatorial Electrojet, Geophys. Res. Lett., 18, 41–44, 1991.

Kudeki, E., Farley, D. T., and Fejer, B. G.: Theory of Spectral Asymetries and Nonlinear Currents in the Equatorial Electrojet, J. Geophys. Res., 90, 429, 1985.

Kudeki, E., Bhattacharyya, S., and Woodman, R. F.: A New Approach in Incoherent Scatter F Region ExB Drift Measurements at Jicamarca, J. Geophys. Res., 104, 28 145–28 162, 1999.

Lagunas, M., Santamaria, M., Gasull, A., and Moreno, A.: Maximun Likelihood Filters in Spectral Estimation Problems, Signal Processing, 10, 19–34, 1986.

Palmer, R. D., Vangal, S., Larsen, M. F., Fukao, S., Nakamura, T., and Yamamoto, M.: Phase calibration of VHF spatial interferometry radars using stellar sources, Radio Sci., 31, 147–156, 1996.

Palmer, R. D., Gopalam, S., Yu, T. Y., and Fukao, S.: Coherent Radar Imaging Using Capon's Method, Radio Sci., 33, 1585–1598, 1998.

Ronchi, C.: Large Scale Turbulence in the Equatorial Electrojet, Ph.D. thesis, Cornell Univ., Ithaca, New York, 1990.

Stoica, P. and Moses, R.: Introduction to Spectral Analysis, Prentice-Hall, Inc., 1997.

Woodman, R. F.: Inclination of the geomagnetic field measured by an incoherent scatter technique, J. Geophys. Res., 76, 178–184, 1971.

Woodman, R. F.: Coherent Radar Imaging: Signal Processing and Statistical Properties, Radio Sci., 32, 2373–2391, 1997.

Yu, T. Y., Palmer, R. D., and Hysell, D. L.: A Simulation Study of Coherent Radar Imaging, Radio Sci., 35, 1129–1141, 2000.